Biochemical Basis for Enhanced Binding of Peptide Dimers to X-Linked Inhibitor of Apoptosis Protein†

Kathryn E. Splan,*,‡ John E. Allen,§ and George L. McLendon*,§

Department of Chemistry, Macalester College, 1600 Grand Avenue, St. Paul, Minnesota 55105, and Department of Chemistry, Duke University, P.O. Box 90317, Durham, North Carolina 27708

Received September 18, 2006; Revised Manuscript Received August 3, 2007

ABSTRACT: XIAP (X-linked inhibitor of apoptosis protein) is involved in the mediation of programmed cell death and, therefore, is a target for the development of cancer therapeutics. Peptide mimetics based upon Smac, the natural binding partner of XIAP, and specifically, dimeric peptides, have shown great promise in drug development. In the present work, the basis for enhanced dimer efficacy has been explored. Comparisons are made between the peptide binding site on the BIR3 domain of XIAP alone (residues 238−358) and a less truncated construct that includes both BIR2 and BIR3 domains (residues 151−350). This contingency differentially enhances the binding of dimeric tetrapeptides, potentially by providing additional hydrophobic binding surface. The effect of BIR2 on the BIR3 binding site is sustained, even if the BIR2 binding site is disrupted by mutagenesis, as shown by both a fluorescent competition assay and a polarity sensitive dye, badan. FRET measurements reveal an observed separation of ≥45 Å between the BIR2 and BIR3 peptide binding pockets, thereby precluding a direct simultaneous interaction of the dimer molecules with both binding domains. Furthermore, variations in the linker length between dimeric tetrapeptides did not show a predictable trend in binding affinities, suggesting that local concentration effects were also an unlikely explanation for the enhanced dimeric affinities. Taken together, the results suggest that enhanced binding of dimeric peptides likely reflects the increased hydrophobic surface area on or near the BIR3 site and have significant ramifications for the design of therapeutics that target this class of proteins.

Apoptosis, or programmed cell death, is an essential process in the development and homeostasis of multicellular organisms (*1*−*3*). As such, disruption of apoptotic pathways can lead to a variety of pathologic conditions, including neurodegenerative diseases, cardiovascular diseases, acquired immunodeficiency syndrome, and cancer. The mechanism of apoptosis is based upon the sequential activation of cysteine proteases, known as caspases, whose proteolytic activity ultimately leads to cell death (*4*, *5*)

The inhibitor of apoptosis proteins (IAPs[1]) play a significant role in the negative regulation of apoptosis by inhibiting the enzymatic activity of caspases (*6*, *7*). All IAPs contain at least one ∼70-residue zinc-binding domain known as the baculovirus IAP repeat (BIR) domain. One of the best-characterized IAPs, human X-linked IAP (XIAP), contains three BIR domains and a C-terminal RING finger. The BIR2 domain and the preceding linker region inhibit caspase-3 and −7 (*8*−*10*), while BIR3 binds and directly inhibits caspase-9 (*11*). The RING domain is an E3 ubiquitin ligase and promotes the proteosomal degradation of several apoptotic proteins (*12*−*14*). Although the function of the BIR1 domain of XIAP is unknown, a recent study indicates that the BIR1 domain of cIAP1 mediates binding to and ubiquitination of TRAF (TNF receptor-associated factor) (*15*).

During the apoptotic cascade, XIAP is normally inhibited by Smac (the secondary mitochondrial activator of caspases) (*16*−*18*). Upon receipt of an apoptotic stimulus, Smac is released from the mitochondria and directly binds to XIAP, resulting in the relief of caspase inhibition. Some forms of cancer show drastically upregulated levels of XIAP, causing cellular levels of Smac to be insufficient to induce apoptosis (*7*, *19*). Therefore, XIAP is an important protein for the development of targeted chemotherapeutics (*20*).

Biochemical, structural, and chemical studies have shown that the basis for Smac binding to the BIR3 domain is Smac's N-terminal tetrapeptide motif (AVPI) (*21*−*23*). Peptide and peptidomimetic structural homologues of AVPI can replace full length Smac in binding to XIAP's BIR3 domain, causing caspase release, as shown in protein and cellular assays (*21*, *24*, *25*). Such studies have created great interest in the development of peptidomimetic leads for drug development. A recent report by Li et al. revealed that tetrapeptide dimers showed significantly improved binding to XIAP and increased caspase activity in cellular assays when compared to the monomeric derivatives (*26*). The authors suggest that

† This work was supported by NIH Grant GM059348 (to G.L.M.).

* Corresponding author. Tel: 919-684-4510. Fax: 919-684-8504. E-mail: george.mclendon@duke.edu (G.L.M.); splank@macalester.edu (K.E.S.).

‡ Macalester College.

§ Duke University.

[1] Abbreviations: IAPs, inhibitor of apoptosis proteins; BIR, baculovirus IAP repeat; XIAP, X-linked inhibitor of apoptosis protein; Smac, secondary mitochondrial activator of caspases; MBHA, methylbenzhydrylamine; HBTU, 2-(1*H*-Benzotriazole-1-yl)-1,1,3,3-tetramethylaminium hexafluorophosphate; Fmoc, fluorenyl-methoxycarbonyl; Boc, butyloxycarbonyl; badan, 6-(bromoacetyl)-2-(dimethylamino)naphthalene; TFA, trifluoracetic acid; DIEA, diisopropylethylamine.

10.1021/bi061938t CCC: $37.00
Published on Web 10/02/2007

Scheme 1: Peptide Compounds Used in This Study

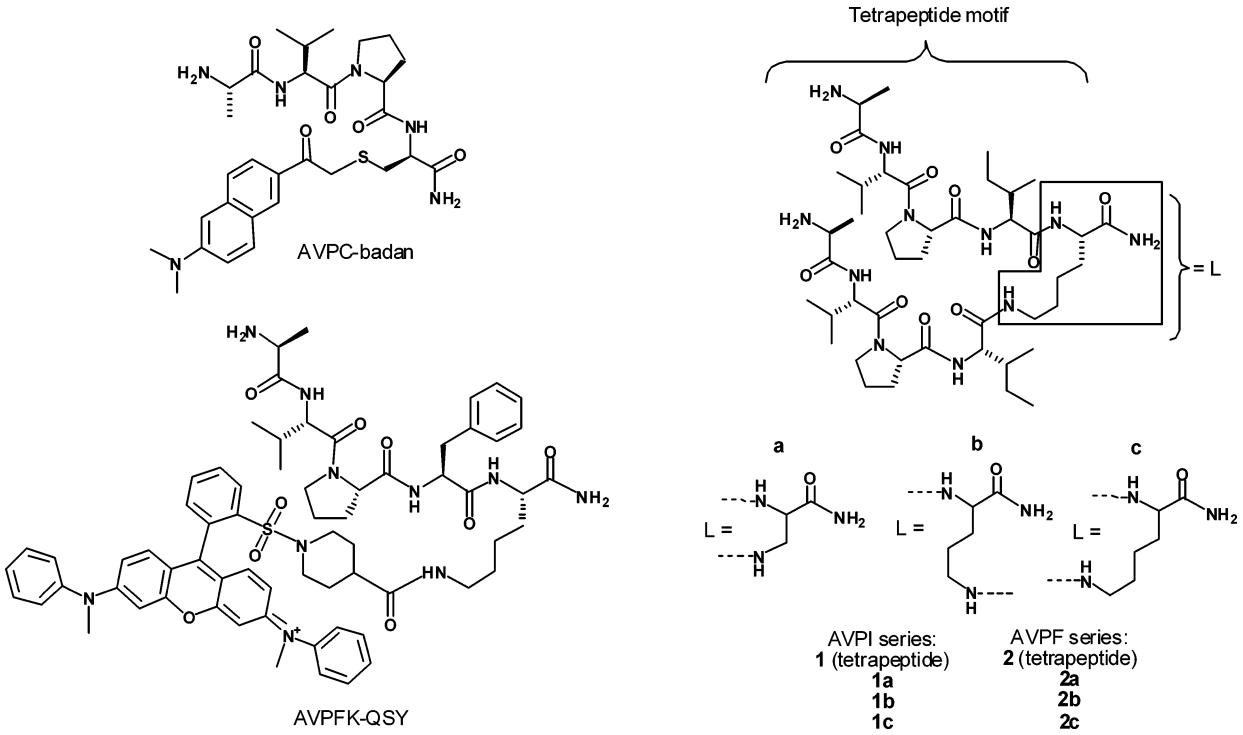

this increased activity may result from dimeric peptides simultaneously binding to the BIR2 and BIR3 domains, in a similar fashion as has been predicted for native Smac (*27*).

While both the isolated BIR2 and BIR3 domains of XIAP have been structurally characterized via NMR and crystallography experiments (*22*, *28*), no structural information is available for full length XIAP. As a result, neither the nature of the BIR2 and BIR3 binding pockets within full length XIAP nor the distance between the two binding sites is known. In the present work, the basis for enhanced dimer efficacy toward XIAP is explored. Comparisons are made between the peptide-binding site on the BIR3 domain alone (residues 238−358) and a less truncated construct that includes both BIR2 and BIR3 domains (residues 151−350; referred to as BIR2_3 throughout). Utilizing an environment-sensitive fluorescent probe, the hydrophobic nature of the binding site is explored, and our studies reveal a significant change in the BIR3 binding site when in the presence of BIR2. Dimeric peptides based upon the Smac tetrapeptide motif are presented (Scheme 1), along with binding data to both BIR3 and BIR2_3. On the basis of fluorescent resonance energy transfer (FRET) measurements, the distance between the BIR2 and BIR3 domains is estimated and found to be significantly larger than the span of the peptide dimers, indicating that simultaneous binding to BIR2 and BIR3 is prohibited. Taken together, the studies reported herein have significant ramifications in the design of therapeutics that target IAPs.

MATERIALS AND METHODS

Materials. Unless otherwise stated, materials were purchased from Aldrich Chemical Co. (Milwaukee, WI) or VWR Scientific and were used without further purification. Methylbenzhydrylamine (MBHA) Rink amide solid-phase peptide synthesis resin, 2-(1*H*-Benzotriazole-1-yl)-1,1,3,3-tetramethylaminium hexafluorophosphate (HBTU), and 9-fluorenyl-methoxycarbonyl- (Fmoc-) protected amino acids were obtained from NovaBiochem (San Diego, CA). 9-[2-[[4-[[(2,5-Dioxo-1-pyrrolidinyl)oxy]carbonyl]-1-piperidinyl]-sulfonyl]phenyl]-3,6-bis(methylphenylamino)-, chloride (QSY), 6-(bromoacetyl)-2-(dimethylamino)naphthalene (badan), and fluorescein-5-maleimide were purchased from Invitrogen (Madison, WI).

Expression and Purification of Truncated XIAP. Recombinant XIAP-BIR3 was overexpressed as a GST fusion protein as described previously (*21*). Wild type and mutant XIAP-BIR2_3 were overexpressed as 6xHis fusion proteins using a pET21b vector (Novagen) in BL21 (DE3) *E. coli*. Transformed cells were grown at 37 °C until O.D. was ∼0.6 and induced with 0.5 mM IPTG overnight at 27 °C. Harvested cells were lysed via sonication and spun at 15,000 rpm for 90 min to remove cell debris. The cleared lysate was loaded onto a Ni-NTA affinity column (Qiagen) and washed with 20 mM imidazole. The desired protein was eluted with 250 mM imidazole, concentrated, and exchanged via ultrafiltration (Amicon) into buffer containing 50 mM potassium phosphate at pH 7.0, 100 mM NaCl, and 2 mM DTT. All protein concentrations were determined via the Bradford method (Bio-Rad). All mutants were generated by site-directed mutagenesis using a QuikChange (Stratagene) mutagenesis kit and were confirmed via DNA sequence determination.

Preparation of Synthetic Peptides. AVPC-badan was prepared as described previously (*21*). Peptide dimers were synthesized by standard Fmoc protocol on MBHA resin utilizing an Advanced ChemTech 396 MPS automated peptide synthesizer (*29*). The lysine derivates ornithine and diaminopropionic acid, in which both the backbone and side chain amines are Fmoc- protected, were chosen as the C-terminal residues to provide the scaffold on which the

dimeric peptides were synthesized. All peptides were cleaved from the resin with 95% trifluoroacetic acid, 2.5% water, and 2.5% triisopropylsilane, and purified via reverse-phase HPLC with gradient elution by solvents A (99% H_2O, 1% CH_3CN, and 0.1% TFA) and B (90% CH_3CN, 10% H_2O, and 0.1% TFA) and subsequently lyophilized. Molecular mass and purity were confirmed via LCMS-ESI.

Synthesis of AVPFK-QSY. The Ala-Val-Pro-Phe-Lys peptide was synthesized using a 1-(4,4-dimethyl-2,6-dioxocyclohex-1-ylidene)ethyl (Dde) group to protect the lysine side-chain amine and a Boc group to protect the N-terminal alanine. Upon completion of the sequence, Dde was removed via reaction with 2% H_2N_2 in DMF (3 × 5 min). QSY-succinimide ester was added and allowed to react overnight in the presence of diisopropylethylamine (DIEA). The peptide was washed to remove excess dye, cleaved from the resin, and purified as described above.

Determination of Dissociation Constants for Peptides. Fluorescence spectra were recorded using a Photon Technologies, Inc. fluorometer with a Xe arc lamp and PMT detector. The absorbance of all solutions was less than 0.1 at the excitation wavelength (387 nm). To determine the binding constants for AVPC-badan to BIR3 and BIR2_3, 1 μM AVPC-badan was titrated with a protein stock solution from 0 to 10 μM. The binding constant was then determined from the intensity measurements at 470 nm after each addition of the protein. Dissociation constants for peptide compounds were determined via competition experiments in which equal molar amounts of AVPC-badan, XIAP, and peptide were incubated and the fluorescence recorded. The fraction of unbound dye in solution was determined from observed intensity at 470 nm and the limiting spectra for both fully bound and free dye. Peptide dissociation constants (K_D) were then calculated from the following expression:

$$K_D = \frac{K_D(forAVPC - badan)}{\left(\frac{[badan_{total}](F_{free})^2}{([peptide_{total}] - [badan_{total}]F_{free})((1 - F_{free}))}\right)} \quad (1)$$

where F_{free} is the fraction of AVPC-badan, which is not bound to the BIR3 domain. F_{free} is defined as follows:

$$F_{free} = \frac{[badan_{free}]}{[badan_{total}]} = \frac{I_{sample} - I_{bound}}{I_{free} - I_{bound}} \quad (2)$$

where I_{free} is the intensity of AVPC-badan alone, I_{bound} is the intensity of AVPC-badan fully bound to BIR3 or BIR2_3, and I_{sample} is the intensity of the specific experimental sample.

FRET Studies. A triple mutant was constructed in which the free cysteine residues C202 and C213 of BIR2_3 were replaced by alanine and glycine, respectively, and E219 in the BIR2 binding pocket was replaced with cysteine. Labeling experiments were carried out in buffer containing 50 mM potassium phosphate (pH 7.2) and 2 mM tris(2-carboxyethyl)phosphine (TCEP). A 50 μM protein solution (250 μL) was reacted overnight at 4 °C with a 10-fold excess of fluorescein-5-maleimide, a thiol-reactive dye. The protein was then passed through a gel-filtration spin column (Pierce) to remove unreacted dye, and further purified via repeated concentration/dilution cycles with a Microcon YM-10 centrifugal filtration device (Millipore). SDS−PAGE confirmed the presence of dye-labeled protein and the absence of residual dye. The fluorescence quantum yield for the dye-labeled protein (ϕ_D) was determined by comparing the integrated fluorescence intensity to that of Rhodamine 6G, on the basis of established procedures (*30*). The optical density for both the protein and standard were kept below 0.06 to avoid inner filter effects. The Förster distance (R_o) was calculated from the overlap integral of the donor emission and acceptor absorption, utilizing the following parameters: $\phi_D = 0.65$, $\kappa^2 = 0.67$, and $n = 1.4$ for a protein solution.

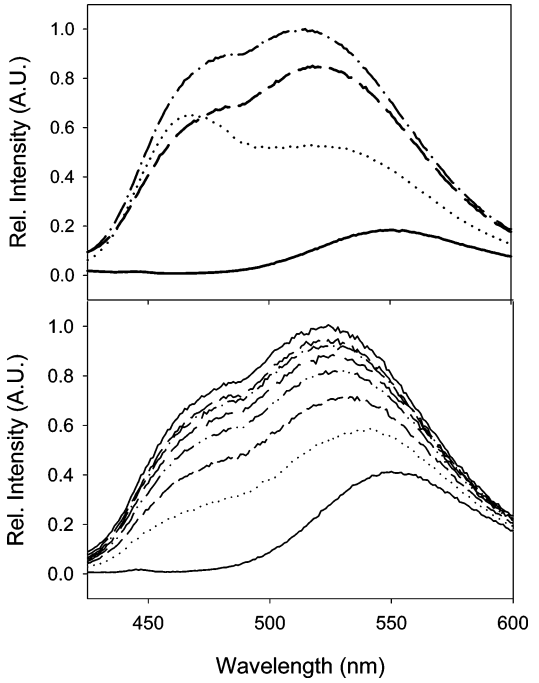

FIGURE 1: (Top) Fluorescence spectra of 1 μM AVPC-badan in the absence of XIAP (—) and in the presence of 20 μM BIR3 (···), BIR2_3 (− −), and BIR2_3_E219C (− · −). (Bottom) Titration of AVPC-badan with BIR2_3.

RESULTS

XIAP's BIR3 Substrate Binding Pocket Is Modified in the Presence of the BIR2 Domain. In earlier work, our laboratory showed that upon binding to the BIR3 domain the peptide reporter AVPC-badan produced a characteristic spectrum (Figure 1, top) which reflected the local polarity and rigidity of the binding site (*21*). Because of the hydrophobic environment of the binding pocket, the spectrum features a dramatic increase in intensity and a blue shift in badan emission c.a. 550 nm. Furthermore, a higher energy localized emission is observed at 470 nm that is characteristic of this class of charge-transfer dyes (*31*). However, binding the same reporter peptide to the BIR3 site in an expanded BIR2_3 construct results in a different spectrum (Figure 1, top). Most notably, the relative intensity of the peaks is reversed, and the band centered at 550 nm is relatively blue-shifted. This observed blue shift in emission is consistent with an increase in the hydrophobic character of the binding site.

While previous studies indicate that BIR3 is a more favorable binding site for Smac peptide mimetics relative to BIR2 (*22*), the observed spectral difference described above could reflect a binding distribution between both the BIR2

Table 1: Dissociation Constants (K_d) for Peptide Compounds and Various XIAP Constructs

compound	BIR3 (nM)	BIR2_3 (nM)	BIR2_3_E219C (nM)
AVPC-badan	3600 ± 700	1700 ± 600	1900
1	300 ± 10	132 ± 89	71 ± 16
1a	132 ± 7	4 ± 3	8 ± 2
1b	87 ± 3	3 ± 2	9 ± 5
1c	119 ± 5	5	n/a
2	25 ± 6	32	11 ± 5
2a	2 ± 1	1.0 ± 0.1	1.1 ± 0.3
2b	7 ± 1	0.9 ± 0.2	2 ± 1
2c	7 ± 1	1.8	1.3 ± 0.4

and BIR3 sites. If both BIR2 and BIR3 sites were partially occupied, at high BIR2_3 concentrations the emission spectrum would be expected to shift toward the characteristic BIR3 spectrum because of its higher affinity for Smac peptides. However, upon titration of AVPC-badan with BIR2_3, the emission spectrum of AVPC-badan maintains a constant line shape, indicative of a single binding site (Figure 1, bottom).

To further distinguish between these possibilities, a modified BIR2_3 construct containing an altered BIR2 binding pocket was prepared. Previous experiments with BIR3 have shown that mutation of the Q319 residue that makes a critical hydrogen bond to the N-terminal alanine of the Smac tetrapeptide motif significantly reduces this interaction (*23*). Therefore, the analogous residue in the BIR2 domain, E219, was replaced by a cysteine residue. In the presence of an excess of this modified protein, AVPC-badan displays an emission spectrum that is essentially equivalent to that of the unmodified BIR2_3 and very different from that of BIR3 alone. This experiment suggests that the BIR2 domain is not directly involved in binding and is consistent with the high affinity of tetrapeptide substrates for the BIR3 binding site versus the substantially lower reported tetrapeptide affinities for the BIR2 binding site. Taken together, the emission spectra of AVPC-badan when bound to wild type and mutant BIR2_3 and BIR3 constructs suggests that the presence of the expanded construct creates a marked change in the environment of the BIR3 binding site.

Dimeric Peptide Binding Is Enhanced in BIR2_3 Constructs. As stated in the Introduction, a previous study reported upon the enhanced efficacy of a Smac mimetic when incorporated into a dimeric structure, and the observed enhancement was attributed to simultaneous interaction with both BIR2 and BIR3 domains (*26*). To further examine the affinity of dimeric peptides based upon the N-terminal sequence of Smac for various XIAP constructs, peptide dimers based upon both the AVPI and AVPF sequences were synthesized via solid-phase peptide synthesis (SPPS). As illustrated in Scheme 1, AVPI and AVPF sequences were built upon various lysine derivatives, resulting in dimeric structures with varying linker lengths. In these structures, while the putative dimeric binding motif (i.e., AVPI) may be thought of as symmetric, it should be noted that the presence of a C-terminal amide functionality results in a loss of overall symmetry.

Table 1 summarizes the binding of peptide monomers and dimers to isolated BIR3 and BIR2_3 constructs measured via competitive displacement of the AVPC-badan probe. While monomer binding increases modestly (3×) in the BIR2_3 construct relative to BIR3, dimer binding is significantly enhanced (10−30×). Furthermore, similar binding constants are observed for both wild type BIR2_3 and a mutated version that contains a disruption within the proposed BIR2 binding cleft. As illustrated above, placing the BIR3 site within an extended construct (presumably more similar to full length XIAP) resulted in a modified site with more hydrophobic character, and it appears that such modification might facilitate the binding of substrates simply by the additional hydrophobic surface.

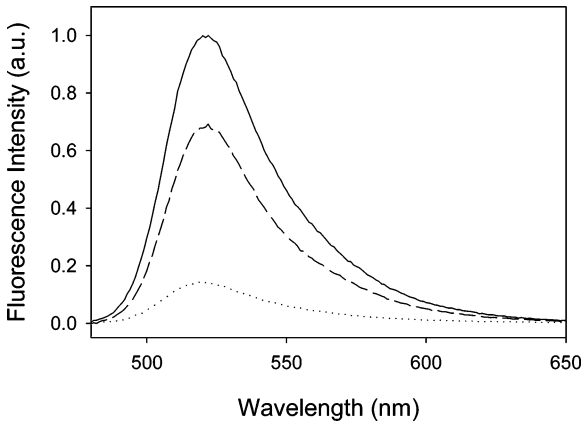

FIGURE 2: Emission spectra of fluorescein-labeled BIR2_3 (0.50 μM) alone (—), in the presence of 2.0 μM AVPFK-QSY (····), and in the presence of both 2.0 μM AVPFK-QSY and 50 μM **2c**.

Measurement of Domain Separation Distance via FRET Measurements. While both the isolated BIR2 and BIR3 domains of XIAP have been structurally characterized, the relative orientation between the domains is unknown. To this end, Förster energy transfer measurements were employed to elucidate the distance between the binding pockets. A triple mutant was constructed in which the free cysteine residues C202 and C213 of BIR2_3 were replaced by alanine and glycine, respectively (*28*), and E219 in the BIR2 binding pocket was replaced with cysteine. This BIR2_3 construct was then reacted with a thiol specific fluorescein derivative to selectively label the BIR2 binding groove. To label the BIR3 binding site with an appropriate acceptor chromophore for fluorescein, the peptide probe AVPFK-QSY (Scheme 1) was synthesized. In addition to exhibiting favorable spectral overlap with fluorescein, QSY is a nonfluorescent quencher, allowing for simplification of data analysis because of the absence of nonsensitized accepter emission. Furthermore, competition assays with AVPC-badan reveal that this probe binds to BIR3 with subnanomolar affinity (data not shown), thereby effectively labeling the BIR3 binding groove even in dilute solutions. The fluorescence quantum yield of fluorescein was measured upon labeling of BIR2_3 to yield a value of 0.65, resulting in an experimental Förster energy transfer radius (R_o) of 57 Å. This value is in good agreement with the reported literature value of 61 Å for this donor−acceptor pair (*32*).

Incubation of the fluorescein-labeled BIR2_3 construct with AVPFK-QSY resulted in 86% quenching of donor emission, attributed to energy transfer quenching by the QSY motif (Figure 2). As a control, when excess unlabeled AVPF peptide was added, fluorescence of the BIR2-fluorescein donor was partially recovered, to 69% of the original value, indicating that a significant portion of the observed quenching

is attributed to energy transfer between the BIR2 pocket and the BIR3 bound peptide. The remainder of the observed quenching is attributed to nonspecific binding because of the extreme hydrophobic nature of the QSY dye. The ratio of the quenched fluorescence intensity to the recovered fluorescence intensity then gives the quenching efficiency attributed to energy transfer between the BIR2 and BIR3 binding pockets, which is calculated to be 0.80.

The relationship between the efficiency of energy transfer (E) and the donor−acceptor distance (R) is given by the following equation:

$$E = \frac{R_o^6}{(R_o^6 + R^6)} \quad (3)$$

where R_o is the Förster distance, or the distance at which energy transfer is 50% efficient. On the basis of eq 3, a quenching efficiency of 0.80 and an R_o value of 57 Å yields a site-to-site distance of 45 Å.

Because steady-state measurements rather than time-resolved techniques were employed, it is not possible to resolve all of the potential distance distributions that may be present due to nonspecific binding of the QSY-acceptor probe. It is therefore acknowledged that the experiments described above only allow for an estimate of the interdomain distance. Molecular modeling of dimer **1c** on the basis of the crystal structure of AVPI bound to BIR3 (*23*) revealed a distance of 26 Å between the terminal alanine residues when the dimer is in its extended conformation. On the basis of the parameters outlined above and the estimated maximum length of the peptide, quenching efficiency from the fluorescein donor to the QSY acceptor would be >99% efficient at this distance. Therefore, we reasoned, anything less than complete quenching is indicative of an intersite distance too large to accommodate multiple site binding.

Enhanced Dimer Binding Does Not Reflect Simple Statistical Arguments. An additional possible source of enhanced binding of tetrapeptide dimers is the local concentration effect. This argument suggests that by covalently constraining a second ligand in close proximity to a bound ligand (peptide), the effective ligand concentration at the moment of dissociation is higher for a dimer relative to a monomer (*33*). Such arguments predict a simple, monotonic decrease in binding affinity as the dimer linker length increases and should hold true for both the isolated BIR3 domain and the larger BIR2_3 construct. This was not observed. Indeed, no correlation was observed between linker length and binding affinity (Table 1).

The simplest explanation for enhanced dimer affinity is that an extended BIR2_3 construct provides some additional hydrophobic surface, which may interact with available hydrophobic residues on the dimer. This is consistent with the observation that although both AVPI and AVPF dimers have greater affinity than their monomeric counterparts, AVPF dimers bind more strongly than AVPI dimers. Since the hydrophobic effect provides approximately 0.8 kcal/mol for each additional carbon atom shielded from water (*34*), modest structural changes could account for the observed magnitude of enhanced dimer binding. The lack of an observable correlation with the linker size argues against a proximal effect, and thus suggests that homodimers are not necessarily an optimal approach to the construction of high affinity binders.

DISCUSSION

IAPs (inhibitor of apoptosis proteins) represent potentially important targets for many types of cancer, where IAP overexpression blocks the cell death pathway. The protein Smac acts by binding to XIAP, thereby releasing caspase 9 to initiate the apoptosis cascade (*11*). Crystallography and NMR studies show that the Smac/IAP interaction is dominated by a simple tetrapeptide sequence, AVPI (*22*, *23*). This finding has facilitated the design and testing of peptide homologues and peptide mimetics that have been shown to be active *in vivo* and *in vitro* (*24*, *25*).

As described above, a potential advance in the design of small molecule Smac mimics was recently reported, illustrating that when Smac mimetic tetrapeptides were dimerized, the binding to IAPs increased dramatically (*26*). This increased affinity was attributed to bivalency, and it was proposed that dimeric Smac mimics might simultaneously bind to both the BIR3 binding site and the corresponding BIR2 site. The results summarized above do not support this model for the peptides described herein. The measured distance between the sites was found to be approximately 45 Å, a distance far too great for a nine amino acid sequence to span, barring a large conformational change. Additionally, dimer binding to a BIR2_3 construct with an altered BIR2 site was not significantly affected.

The possibility of binding enhancement as a result of effective local concentration was tested by varying the dimer's linker length. However, if this were true, the apparent binding constants should have decreased as the chain length of the linker increased (corresponding to an increase in effective volume, with a corresponding decrease in effective concentration). There was no evidence for such an effect on the basis of the data shown in Table 1.

These findings suggest that the BIR3 domain is the sole target of the Smac-based dimeric peptide inhibitors examined herein. When the BIR3 domain is incorporated into a larger BIR2_3 construct, the larger construct subtly alters the BIR3 binding site to increase its hydrophobic binding propensity. It appears that the increased activity of the dimers is proportional to their ability to make full use of the available hydrophobic sites.

An aspect not considered in this study is the oligomerization state of XIAP. The BIR motifs of the IAP proteins Op-IAP (*35*) and Survivin (*36*) have been shown to induce self-oligomerization, while the RING finger domain promotes the self-association of XIAP (*37*). Furthermore, structural studies reveal that Smac, the natural binding partner of XIAP, is homodimeric (*16*). While a mutant Smac monomer is sufficient for interaction with the isolated XIAP BIR3 domain, interaction with BIR2 requires the dimeric structure, suggesting that BIR2 might dimerize in solution (*16*). However, an alternate mode of binding for Smac proposes simultaneous interaction with both BIR2 and BIR3 domains, which would argue against the necessity for oligomerization for this interaction (*27*).

While the results reported herein rule out a direct simultaneous interaction of the dimer molecules with both BIR2 and BIR3 domains, the data is not inconsistent with

the formation of an XIAP dimeric complex wherein the peptide dimers span two BIR3 domains. The possibility of BIR2-induced dimerization of XIAP may contribute to the enhanced binding of dimers relative to monomers by placing two (or more) BIR3 binding pockets in close proximity. To explore this mode of binding, detailed studies utilizing size exclusion chromatography and ultracentrifugation will be undertaken to directly observe a possible multi-protein complex. Studies of this type will provide valuable insight into the mechanism by which small molecule therapeutics interact with XIAP.

CONCLUSIONS

In conclusion, we have shown that upon incorporation into a larger XIAP construct, the hydrophobic nature of the BIR3 binding site is altered, as evidenced by fluorescence spectral data. It was found that dimeric peptides based upon Smac, the natural binding partner for XIAP, have a considerably higher affinity for XIAP constructs containing both BIR2 and BIR3 domains, relative to the isolated BIR3. Förster energy transfer experiments estimate the distance between the two binding sites to be ≥45 Å, thereby indicating that such dimeric motifs cannot bind to both domains simultaneously, as was previously predicted. As a result, the concept of effective dimeric Smac mimetics is challenged, and alternative structures for effective therapeutics must be pursued.

ACKNOWLEDGMENT

We thank Ms. Kim Steward for helpful discussions and Dr. Yigong Shi for providing the plasmid for XIAP BIR2_3.

REFERENCES

1. Green, D. R. (2000) Apoptotic pathways: Paper wraps stone blunts scissors, *Cell 102*, 1−4.
2. Shi, Y. (2001) A structural view of mitochondria-mediated apoptosis, *Nature Struct. Biol. 8*, 394−401.
3. Fesik, S. W. (2000) Insights into programmed cell death through structural biology, *Cell 103*, 273−282.
4. Thornberry, N. A., and Lazebnik, Y. (1998) Caspases: enemies within, *Science 281*, 1312−1316.
5. Wolf, B. B., and Green, D. R. (1999) Suicidal tendencies: Apoptotic cell death by caspase family proteinases, *J. Biol. Chem. 274*, 20049−20052.
6. Deveraux, Q. L., and Reed, J. C. (1999) IAP family proteins: suppressors of apoptosis, *Genes Dev. 13*, 239−252.
7. LaCasse, E. C., Baird, S., Korneluk, R. G., and Mackenzie, A. E. (1998) The inhibitors of apoptosis (IAPs) and their emerging role in cancer, *Oncogene 17*, 3247−3259.
8. Chai, J., Shiozaki, E., Srinivasula, S. M., Wu, Q., Dataa, P., Alnemri, E. S., and Shi, Y. (2001) Structural basis of caspase-7 inhibition by XIAP, *Cell 104*, 769−780.
9. Riedl, S. J., Renatus, M., Schwarzenbacher, R., Zhou, Q., Sun, C., Fesik, S. W., Liddington, R. C., and Salveson, G. S. (2001) Structural basis for the inhibition of caspase-3 by XIAP, *Cell 104*, 791−800.
10. Scott, F. L., Denault, J. B., Riedl, S. J., Shin, H., Renatus, M., and Salvesen, G. S. (2005) XIAP inhibits caspase-3 and -7 using two binding sites: Evolutionarily conserved mechanism of IAPs. *EMBO J. 24*, 645−655.
11. Srinivasula, S. M., Hegde, R., Saleh, A., Datta, P., Shiozaki, E., Chai, J. J., Lee, R. A., Robbins, P. D., Fernandes-Alnemri, T., Shi, Y., and Alnemri, E. S. (2001) A conserved XIAP-interaction motif in caspase-9 and Smac/DIABLO regulates caspase activity and apoptosis, *Nature 410*, 112−116.
12. Huang, H. K., Joazeiro, C. A. P., Bonfoco, E., Kamada, S., Leverson, J. D., and Hunter, T. (2000) The inhibitor of apoptosis, cIAP2, functions as a ubiquitin-protein ligase and promotes in vitro monoubiquitination of caspases 3 and 7, *J. Biol. Chem. 275*, 26661−26664.
13. Yang, Y., Fang, S. Y., Jensen, J. P., Weissman, A. M., and Ashwell, J. D. (2000) Ubiquitin protein ligase activity of IAPs and their degradation in proteasomes in response to apoptotic stimuli, *Science 288*, 874−877.
14. Vaux, D. L., and Silke, J. (2005) IAPs, rings and ubiquitylation, *Nat. Rev. Mol. Cell Biol. 6*, 287−297.
15. Samuel, T., Welsh, K., Lober, T., Togo, S. H., Zapata, J. M., and Reed, J. C. (2006) Distinct BIR domains of cIAP1 mediate binding to and ubiquitantion of tumor necrosis factor receptor-associated factor 2 and second mitochondrial activator of caspases, *J. Biol. Chem. 281*, 1080−1090.
16. Chai, J., Du, C., Wu, J. W., Kyin, S., Wang, X., and Shi, Y. (2000) Structural and biochemical basis of apoptotic activation by Smac/DIABLO, *Nature 406*, 855−862.
17. Du, C. Y., Fang, M., Li, Y. C., Li, L., and Wang, X. D. (2000) Smac, a mitochondrial protein that promotes cytochrome c-dependent caspase activation by eliminating IAP inhibition, *Cell 102*, 33−42.
18. Verhagen, A. M., Ekert, P. G., Pakusch, M., Silke, J., Connolly, L. M., Reid, G. E., Moritz, R. L., Simpson, R. J., and Vaux, D. L. (2000) Identification of DIABLO, a mammalian protein that promotes apoptosis by binding to and antagonizing IAP proteins, *Cell 102*, 43−53.
19. Tamm, I., Kornblau, S. M., Segall, H., Krajewski, S., Welsh, K., Kitada, S., Scudiero, D. A., Tudor, G., Qui, Y. H., Monks, A., Andreeff, M., and Reed, J. C. (2000) Expression and prognostic significance of IAP-family genes in human cancers and myeloid leukemias, *Clin. Cancer Res. 6*, 1796−1803.
20. Schimmer, A. D., Dalili, S., Batey, R. A., and Riedl, S. J. (2006) Targeting XIAP for the treatment of malignancy, *Cell Death Differ. 13*, 179−188.
21. Kipp, R. A., Case, M. A., Wist, A. D., Cresson, C. M., Carrell, M., Griner, E., Wiita, A., Albiniak, P. A., Chai, J., Shi, Y., Semmelhack, M. F., and McLendon, G. L. (2002) Molecular targeting of inhibitor of apoptosis proteins based on small molecule mimics of natural binding partners, *Biochemistry 41*, 7344−7349.
22. Liu, Z., Sun, C., Olejniczak, E. T., Meadows, R. P., Betz, S. F., Oost, T., Herrman, J., Wu, J. C., and Fesik, S. W. (2000) Structural basis for binding of Smac/DIABLO to the XIAP BIR3 domain, *Nature 408*, 1004−1008.
23. Wu, G., Chai, J., Suber, T. L., Wu, J. W., Du, C., Wang, X., and Shi, Y. (2000) Structural basis of IAP recognition by Smac/DIABLO, *Nature 408*, 1008−1012.
24. Oost, T. K., Sun, C., Armstrong, R. C., Al-Assad, A. S., Betz, S. F., Deckwerth, T. L., Ding, H., Elmore, S. W., Meadows, R. P., Olejniczak, E. T., Aleksijew, A., Oltersdorf, T., Rosenberg, S. H., Shoemaker, A. R., Tomaselli, K. J., Zou, H., and Fesik, S. W. (2004) Discovery of potent antagonists of the antiapoptotic protein XIAP for the treatment of cancer, *J. Med. Chem. 47*, 4417−4426.
25. Sun, H., Nikolovska-Coleska, Z., Yang, C. Y., Xu, L., Tomita, Y., Krajewski, K., Roller, P. P., and Wang, S. (2004) Structure-based design, synthesis, and evaluation of conformationally constrained mimetics of the second mitochondria-derived activator of caspase that target the X-linked inhibitor of apoptosis Protein/caspase-9 interaction site, *J. Med. Chem. 47*, 4147−4150.
26. Li, L., Thomas, R. M., Suzuki, J., DeBrabander, J. K., Wang, X., and Harran, P. G. (2004) A small molecule Smac mimic potentiates TRAIL- and TNFalpha-mediated cell death, *Science 305*, 1471−1474.
27. Huang, Y., Rich, R. L., Myszka, D. G., and Wu, H. (2003) Requirement of both the second and third BIR domains for the relief of X-linked Inhibitor of Apoptosis Protein (XIAP)-mediated caspase inhibition by Smac, *J. Biol. Chem. 278*, 49517−49522.
28. Sun, C., Cai, M., Gunasekera, A. H., Meadows, R. P., Waant, H., Chen, J., Zhang, H., Wu, W., Xu, N., ng, S. C., and Fesik, S. W. (1999) NMR structure and mutagenesis of the inihibitor-of-apoptosis protein XIAP, *Nature 401*, 818−822.
29. Chan, W. C., and White, P. D. (2000) *Fmoc Solid-Phase Peptide Synthesis: A Practical Approach*, Oxford University Press, Oxford, U.K.
30. Lakowicz, J. R. (2006) *Principles of Fluorescence Spectroscopy*, 3rd ed., Springer, New York.
31. Nitz, M., Mezo, A. R., Ali, M. H., and Imperiali, B. (2002) Photoinduced charge separation via twisted internal charge transfer states, *Chem. Commun.* 1912−1913.

32. *The Handbook: A Guide to Fluorescent Probes and Labeling Technologies* (2006) 10th ed., Invitrogen, Carlsbad, CA.
33. Kiessling, L. L., Gestwicki, J. E., and Strong, L. E. (2000) Synthetic multivalent ligands in the exploration of cell-surface interactions, *Curr. Opin. Chem. Biol. 4*, 696−703.
34. Reynolds, J. A., Gilbert, D. B., and Tanford, C. (1974) Empirical correlation between hydrophobic free energy and aqueous cavity surface area, *Proc. Nat. Acad. Sci. U.S.A. 71*, 2925−2927.
35. Hozak, R. R., Manji, G. A., and Friesen, P. D. (2000) The BIR motifs mediate dominant interference and oligomerization of inhibitor of apoptosis Op-IAP, *Mol. Cell. Biol. 20*, 1877−1885.
36. Verdecia, M. A., Huang, H., Dutil, E., Kaiser, D. A., Hunter, T., and Noel, J. P. (2000) Structure of the human anti-apoptotic protein survivin reveals a dimeric arrangement, *Nature Struct. Biol. 7*, 602−608.
37. Silke, J., Hawkins, C. J., Ekert, P. G., Chew, J., Day, C. L., Pakusch, M., Verhagen, A. M., and Vaux, D. L. (2002) The anti-apoptotic activity of XIAP is retained upon mutation of both the caspase 3- and caspase 9-interacting sites, *J. Cell Biol. 157*, 115−124.

BI061938T